Biocatalytic Photosynthesis Hot Paper

International Edition: DOI: 10.1002/anie.201611379
German Edition: DOI: 10.1002/ange.201611379

Photoelectrochemical Reduction of Carbon Dioxide to Methanol through a Highly Efficient Enzyme Cascade

Su Keun Kuk[+], Raushan K Singh[+], Dong Heon Nam, Ranjitha Singh, Jung-Kul Lee, and Chan Beum Park**

Abstract: *Natural photosynthesis is an effective route for the clean and sustainable conversion of CO_2 into high-energy chemicals. Inspired by the natural process, a tandem photoelectrochemical (PEC) cell with an integrated enzyme-cascade (TPIEC) system was designed, which transfers photogenerated electrons to a multienzyme cascade for the biocatalyzed reduction of CO_2 to methanol. A hematite photoanode and a bismuth ferrite photocathode were applied to fabricate the iron oxide based tandem PEC cell for visible-light-assisted regeneration of the nicotinamide cofactor (NADH). The cell utilized water as an electron donor and spontaneously regenerated NADH. To complete the TPIEC system, a superior three-dehydrogenase cascade system was employed in the cathodic part of the PEC cell. Under applied bias, the TPIEC system achieved a high methanol conversion output of 220 $\mu M\, h^{-1}$, 1280 $\mu mol\, g^{-1}\, h^{-1}$ using readily available solar energy and water.*

Photosynthesis occurs in green plants through a highly efficient, photoinduced energy-transfer cascade consisting of the Z-scheme and the Calvin cycle. The beauty of this natural process has inspired many researchers to develop eco-friendly, solar reductions of CO_2 to hydrocarbon fuels.[1] Methanol, a useful reduced form of CO_2,[2] can be synthesized from CO_2 by the use of different types of photo- or electrochemical catalysts, such as metal complexes and oxide-based semiconductors.[3] These catalysts, however, exhibit critical problems: for example, metal complexes often suffer from severe photocorrosion in an aqueous medium when illuminated by light,[4] while semiconductors generate low yields with poor selectivity and require harsh conditions such as high temperatures and pressures for better output. Recently, redox biocatalysts have been utilized for the photochemical reduction of CO_2. These biocatalysts have several advantages, including the ability to function under mild conditions with extremely high specificity without side reactions, although they suffer from issues of high production cost, poor stability under harsh conditions, and O_2 sensitivity.[5] In principle, a cascade involving three different enzymes, namely formate dehydrogenase (FDH), formaldehyde dehydrogenase (FaldDH), and alcohol dehydrogenase (ADH), can reduce CO_2 to formate, formaldehyde, and methanol in a stepwise manner. However, each of the energetically uphill reductions requires the supply of a stoichiometric amount of expensive nicotinamide cofactor (NADH) to achieve catalytic turnover, and the biocatalytic photochemical systems reported to date for the conversion of CO_2 into methanol are limited by their low yields of NADH regeneration.

Here, we report an inorganic/bioorganic hybrid photosynthetic platform consisting of an NADH-regenerating photoelectrochemical (PEC) cell and a multienzyme cascade (Scheme 1). The tandem PEC cell with an integrated enzyme-cascade (TPIEC) system mimics the natural photosynthetic Z-scheme by acquiring photogenerated electrons from the oxidation of water on illumination with visible light and transferring them to the enzyme cascade for the biocatalytic reduction of CO_2 to methanol. In the photoelectrode-type Z-scheme system, the anodic and cathodic photoelectrodes are separated into two compartments by an ion-exchange salt bridge and connected by a conducting wire to prevent product

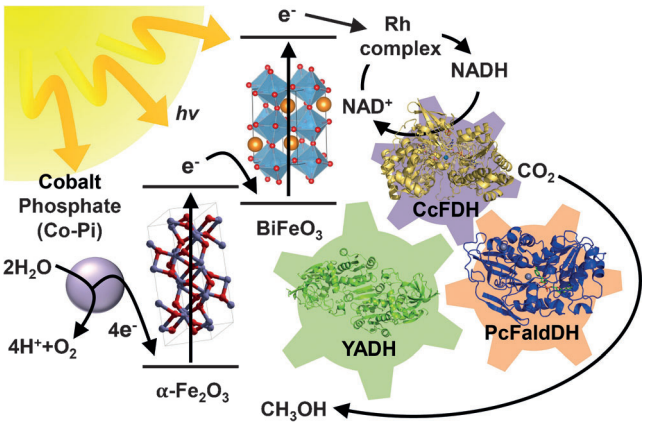

Scheme 1. Schematic illustration of the solar-assisted production of methanol from CO_2 and water through a three-enzyme (CcFDH, PcFaldDH, YADH) cascade. Under illumination by visible light, water is oxidized at the photoanode (Co-Pi/α-Fe_2O_3) and serves as an electron donor. Photoexcited electrons are transferred to the photocathode ($BiFeO_3$), followed by reduction of NAD^+ to NADH via a rhodium-based mediator (**M** = $[Cp^*Rh(bpy)H_2O]^+$, $Cp^* = C_5Me_5$, bpy = 2,2′-bipyridine). Ultimately, the excited electrons from reduced NAD^+ are delivered to the three-enzyme cascade for the biocatalytic synthesis of methanol.

[*] S. K. Kuk,[+] Dr. D. H. Nam, Prof. Dr. C. B. Park
Department of Materials Science and Engineering
Korea Advanced Institute of Science and Technology
335 Science Road, Daejeon 305-701 (Republic of Korea)
E-mail: parkcb@kaist.ac.kr

Dr. R. K. Singh,[+] R. Singh, Prof. Dr. J. K. Lee
Department of Chemical Engineering, Konkuk University
120 Neungdong-ro, Seoul 143-701 (Republic of Korea)
E-mail: jkrhee@konkuk.ac.kr

[+] These authors contributed equally to this work.

Supporting information and the ORCID identification number(s) for the author(s) of this article can be found under: http://dx.doi.org/10.1002/anie.201611379.

mixing and side reactions, a feature which is advantageous for "biocatalyst-based" Z-scheme PEC systems because separated cells allow biocatalysts to maintain their optimal activities.[6] Furthermore, the separation of the anodic and cathodic reactions (i.e. water oxidation reaction and biocatalytic methanol synthesis) can avoid potential damage to anaerobic enzymes from the oxygen-evolving reaction and reoxidation of formate (an intermediate product) at the Co-Pi photoanode. We conducted in situ NADH regeneration using a Co-Pi/α-Fe_2O_3 photoanode and a ferroelectric $BiFeO_3$ photocathode. The photoanode takes up electrons from the water oxidation, and the photocathode transports the electrons to an electron mediator **M** ($[CpRh(bpy)(H_2O)]^{2+}$) and NAD^+ through an internal electric field induced by remnant polarization to regenerate the enzymatically active 1,4-NADH. We reduced CO_2 to methanol in the photocathodic compartment, which contains the FDH-FaldDH-ADH enzyme cascade. In this cascade, FaldDH is a rate-limiting enzyme because of its low catalytic activity during the reduction of formate to formaldehyde. To overcome this limitation, we identified *Pseudomonas cepacia* genomvar II FaldDH (PcFaldDH) by a sequence comparison based on the Basic Local Alignment Search Tool (BLAST), systematic sequence analysis of 100 formate-assimilating microorganisms (see Table S1), and testing of the formate reduction capacity of 30 FaldDHs (see Table S2). We demonstrated that the formate-reducing PcFaldDH shows a high binding affinity to formate and high formate reduction activity, which significantly enhances the rate of conversion of CO_2 into methanol.

For efficient photoelectrochemical regeneration of NADH, we designed an α-Fe_2O_3|$BiFeO_3$ tandem PEC array. α-Fe_2O_3, an n-type semiconductor, was chosen as a photoanode material because its optical band gap (ca. 2.1 eV) provides respectable photocurrents under irradiation with solar light ($\lambda > 420$ nm).[7] $BiFeO_3$, a p-type perovskite semiconductor, is a ferroelectric material that exhibits a band gap of approximately 2.2 eV as well as enhanced photocurrent generation and charge transfer from the electrode to the electrolyte in response to a polarization-induced internal electric field.[8] These two iron oxide materials are stable and show suitable alignment of their band edges within the energy ranges of each electrode, which can pump electrons up to a higher potential simultaneously under irradiation with visible light. We prepared a Co-Pi/α-Fe_2O_3 photoanode with a band gap of 2.18 eV (see Figures S1 and S2) by a solution-based method.[7b] Under alkaline conditions (pH 12), the Co-Pi/α-Fe_2O_3 thin film achieved an anodic photocurrent density 3.2 times higher (1.7 mA cm^{-2}) at 0.6 V (versus Ag/AgCl) than that of bare hematite (Figure 1 a).

A 300-nm-thick polycrystalline $BiFeO_3$ photocathode was prepared by a spin-coating method.[8a] This photocathode exhibits a suitable band gap for the absorption of visible light (2.32 eV, see Figure S3). Polarization-electric (P-E) hysteresis loop tests on $BiFeO_3$ photocathodes showed that the internal electric field of spin-coated $BiFeO_3$ films can be controlled by poling treatment (see Figure S4). Moreover, the application of a +8 V external electric field induced remnant polarization

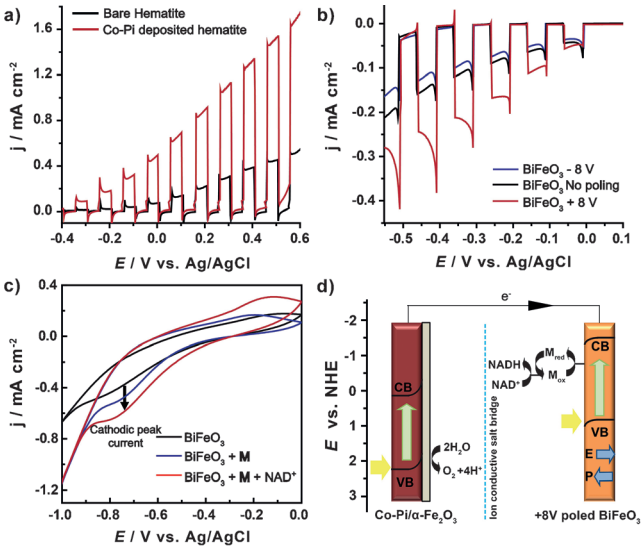

Figure 1. a) Linear sweep voltammetry (LSV) scans of bare hematite and hematite with deposited Co-Pi under chopped light illumination using a three-electrode configuration setup (pH 12). b) LSV scans of a thin film of $BiFeO_3$ before and after poling at +8 V or −8 V under chopped light illumination (pH 7). c) Cyclic voltammogram (CV) curves of a thin film of $BiFeO_3$ poled at +8 V in the absence and presence of **M** and NAD^+ at pH 7. d) Illustration of the Co-Pi/α-Fe_2O_3|$BiFeO_3$ tandem PEC cell for the NADH regeneration system with visible light. The remnant polarization inside the $BiFeO_3$ film induced the internal electric field, which promotes charge separation.

very efficiently. According to the literature, the remnant polarization should generate an internal electric field that induces accumulation of surface charge and drives an upward bending of the energy band of the $BiFeO_3$ film.[8] Upward bending of the energy band inhibited recombination of the photogenerated electron-hole pair and expedited electron transfer toward the electrolyte. As shown in Figure 1 b, the bending of the energy band derived from poling treatment affected the photocurrent of the $BiFeO_3$ photocathodes: the $BiFeO_3$ films poled at +8 V achieved 0.24 mA cm^{-2} at −0.4 V (versus Ag/AgCl), which is 1.6 times greater than that without polarization. In contrast, the photoresponse of the $BiFeO_3$ films was reduced after poling at −8 V. To explore the photogenerated electron transfer from the $BiFeO_3$ photocathode to **M** and NAD^+, we constructed cyclic voltammogram (CV) curves of $BiFeO_3$ electrodes poled at +8 V under a cathodic potential and with **M** and NAD^+ (Figure 1 c). Electron transfer from the photocathode to **M** and NAD^+ was confirmed by enhancement of the cathodic peak current and a potential shift, in agreement with the literature.[9] In the presence of both **M** and NAD^+, the generation of photocurrent at the cathodic peak increased from −0.38 to −0.6 mA cm^{-2} as a result of the reduction of NAD^+ by **M**.

The relationship between the energy band edges of the photoanode, photocathode, and electron mediator **M** plays an important role in the design of tandem PEC cells.[10] The valence band maximum (VBM) and conduction band minimum (CBM) of the $BiFeO_3$ film were calculated to be 0.82 and −1.5 eV, respectively (versus Ag/AgCl), according to analysis by ultraviolet photoelectron spectroscopy (see Fig-

ure S5). The VBM of $BiFeO_3$ was higher than the conduction band edge of hematite, and its CBM was lower than the reduction potential of the electron mediator **M** (−0.73 V versus Ag/AgCl) that transfers hydride ions to NAD^+. These edge configurations of the energy band indicate that $BiFeO_3$ is a proper photocathode material in the tandem PEC cell for in situ regeneration of NADH under irradiation by visible light (Figure 1d). The cathodic current from poled $BiFeO_3$ was lower than the anodic current (see Figure S6), thus implying that $BiFeO_3$ was a current-limiting component in the tandem PEC cell. Without applied voltage, a spontaneous current of approximately 100 $\mu A\,cm^{-2}$ was predicted from the overlap onset potential of each photoelectrode under irradiation with visible light.

We assembled the Co-Pi/α-Fe_2O_3 | $BiFeO_3$ tandem PEC NADH regeneration system in a two-electrode configuration containing Co-Pi/α-Fe_2O_3 as a working electrode and $BiFeO_3$ as a counter electrode under ambient conditions with visible light. The two-component cell was separated into an oxygen-evolving reaction (anodic) part and a photobiocatalytic methanol-formation (cathodic) part. The photoanode was employed under alkaline conditions (pH 12), thereby inducing the oxidation of water (see Figure S7). Enzymes were applied with the photocathode at the optimal pH value (pH 7) and shielded from oxygenic reactions, which could damage metal ions (Zn or W) or iron sulfur clusters of enzyme reaction centers. The difference in the pH values between the two compartments in the tandem PEC cell causes a chemical bias in the PEC system (0.059 V per pH unit, 0.295 V), which drives the electron transfer from the photoanode to the photocathode. The two separated cells were connected by a salt bridge to complete the ionic circuit of tandem cell. Figure 2a shows linear sweep voltammetry scans for each photoelectrode of the tandem PEC cell under visible light. Without irradiation of α-Fe_2O_3 by light, no current passed through the tandem PEC cell, while further irradiation of the $BiFeO_3$ photocathode increased the photocurrent. This observation indicates that the PEC reaction driven by the photoanode was further enhanced by electron excitation at the electric-poled $BiFeO_3$ photocathode. In the case of the illumination of both electrodes by light, a spontaneous photocurrent of 38.3 $\mu A\,cm^{-2}$ was generated with an open circuit voltage of 909.2 mV (see Figure S8). This photocurrent was lower than the predicted value and attributed to ohmic loss in the ionic pathway of the circuit through the salt bridge and electrolyte.[10b,11]

We estimated the efficiency of the NADH-regenerating Co-Pi/α-Fe_2O_3 | $BiFeO_3$ tandem PEC cell in the two-electrode platform by calculating the external applied bias photon to current efficiency (EABPE). In the NADH regeneration system, we defined EABPE according to the following equation: $EABPE = |j| \times (V_{th} - V_{chem} - V_{bias}) \times P_{total}^{-1}$. Note that V_{th} is a theoretical voltage difference between the electrolysis potential of water and the reduction potential of **M** (1.76 V), and V_{chem} is a chemical bias between the two chambers (0.295 V). The best EABPE (0.24%) was obtained at an applied electrical bias of 0.73 V for the NADH-regenerating tandem PEC cell (Figure 2b). We applied the tandem PEC cell to the regeneration of NADH from NAD^+

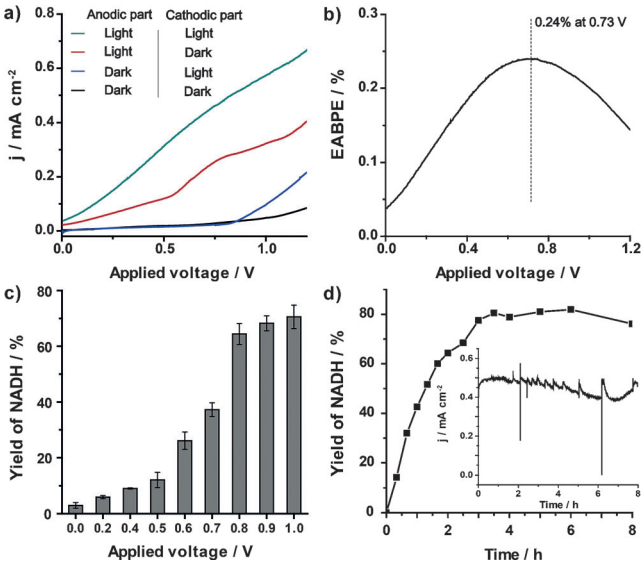

Figure 2. a) Photocurrent response in a two-electrode configuration with Co-Pi/α-Fe_2O_3 (pH 12) and $BiFeO_3$ (pH 7) as a function of the applied voltage under various irradiation conditions (active surface area: 1 cm^2). b) Corresponding EABPE of the Co-Pi/α-Fe_2O_3 | $BiFeO_3$ tandem PEC cell. c) Regeneration yield of NADH by the Co-Pi/α-Fe_2O_3 | $BiFeO_3$ tandem PEC cell as a function of the applied voltage. d) Time profiles of the NADH-regenerating PEC cell under constant electrical bias (0.8 V) over 8 h with illumination by visible light. Inset: chronoamperogram of the PEC cell.

at various applied voltages in the presence of the electron mediator (**M**) and illumination by light for 2 h (Figure 2c). We measured the concentrations of NADH through its absorption at $\lambda = 340$ nm by using a UV spectrophotometer. Under the chemical-biased conditions (without applied voltage), the tandem PEC cell showed a 3% spontaneous regeneration of NADH through the PEC platform. As the applied voltage between the two photoelectrodes increased to 1 V, the yield of NADH regeneration increased up to 70.54% (see Figure S9). At an applied electrical bias of over 0.8 V, the efficiency of the NADH regeneration increased significantly, consistent with the EABPE.

We further investigated the performance and stability of the NADH-regenerating tandem PEC cell under continuous illumination of visible light at an external bias of 0.8 V. A photocurrent of approximately 0.48 $mA\,cm^{-2}$ was observed with good stability during the 8 h reaction, and resulted in an 80% yield for NADH regeneration with 90% of the initial current density retained during the reaction (Figure 2d, Figure S10). To confirm that the photocurrent of the integrated PEC cell originated from the oxidation of water on the α-Fe_2O_3 photoanode, we measured the amount of evolved O_2 on the photoanodic part at an external bias of 0.8 V by using a calibrated fluorescence-based oxygen sensor. From Figure S11 and Figure 2d, the corresponding rates for product generation and faradic efficiencies were estimated to be 4.08 $\mu mol\,h^{-1}$, 94.1% for O_2 evolution, and 7.26 $\mu mol\,h^{-1}$, 88.4% for NADH regeneration. We attribute the reasons why the faradaic efficiencies were less than 100% to hole consumption on the photoanode,[12] electron losses arising from photodegradation of the $BiFeO_3$ photocathode, and

multiple electron-transfer steps in the cathodic compartment. The faradaic efficiencies of approximately 90% and a nearly 2:1 ratio of the rates of NADH regeneration and O_2 evolution indicate that most of the photogenerated electrons generated from the oxidation of water in the photoanode were used for the regeneration of NADH in the photocathode. These results suggest that the Co-Pi/α-Fe_2O_3 | $BiFeO_3$-integrated PEC cell is a highly efficient solar-to-NADH regeneration system that utilizes earth-abundant iron oxide based materials.

To construct the TPIEC system based on the Co-Pi/α-Fe_2O_3 | $BiFeO_3$-integrated PEC cell, we designed a novel enzymatic reaction platform involving a cascade of three dehydrogenases (i.e. FDH, FaldDH, and ADH). PcFaldDH, which encodes a polypeptide of 399 amino acids, was cloned, overexpressed, and purified (see Figure S12 in the Supporting Information). The protein yield of PcFaldDH was estimated to be 41 mg per liter of culture. PcFaldDH belongs to the zinc-containing, medium-chain alcohol dehydrogenase family; it contains two zinc ions per subunit, one catalytic and one structural (Figure 3a). The catalytic zinc center is coordinated by three residues (C47, H68, and D170; Figure 3b). Under optimum conditions, the apparent formate to formaldehyde reduction activity (k_{cat}) of purified PcFaldDH was 0.653 s^{-1} (Table S3, Figure S13). In contrast, PpFaldDH, which is a commercial FaldDH, showed no detectable reduction activity. To the best of our knowledge, PcFaldDH is the first FaldDH enzyme with evident activity for the reduction of formate. To further investigate the ability of PcFaldDH to reduce formate, we performed bioelectrochemical analysis as previously described.[13] The linear sweep voltammetry curve of a porous carbon felt electrode with adsorbed PcFaldDH (Figure 3c) showed a huge formate reduction peak of −1.37 mA cm^{-2} compared to with PpFaldDH (−0.16 mA cm^{-2}). This result shows that PcFaldDH possesses high catalytic activity for formate reduction which can improve the rate-determining step in the enzyme taking part in the methanol cascade. To elucidate the interaction between PcFaldDH and ligands (i.e. formate and NADH), we performed isothermal titration calorimetry (ITC; see Figure S14 and Table S4). The binding constants (K_d values) of formate and NADH to PcFaldDH were 6.20 and 0.67 μM, respectively. These results strongly suggest that PcFaldDH is a suitable biocatalyst that can improve the rate of CO_2 to methanol conversion in a multienzyme cascade system.

To build a methanol-producing, multienzymatic cascade system, we adopted FDH from *Clostridium carboxidivorans* P7T (CcFDH)[14] (see Figures S15 and S12) and the commercial enzyme YADH, along with PcFaldDH. The protein yield of CcFDH was estimated to be 27 mg per liter of culture. CcFDH displayed better catalytic activity and binding constants than the commercial enzyme CbFDH for the reduction of CO_2 (see Figures S14 and S17). In collaboration with PcFalDH, CcFDH converted CO_2 sequentially into formate and then into formaldehyde (see Figures S18–S20). Compared to other multienzyme cascades, the CcFDH-PcFaldDH-YADH cascade system showed superior activity for the CO_2 to methanol conversion (Figure 3d). Individual replacement of CcFDH and PcFaldDH in the cascade reaction resulted in a 3.4- and 5.6-fold increase in the production of methanol, respectively. This finding indicates that PcFaldDH plays a crucial role in the reduction of CO_2 to methanol.

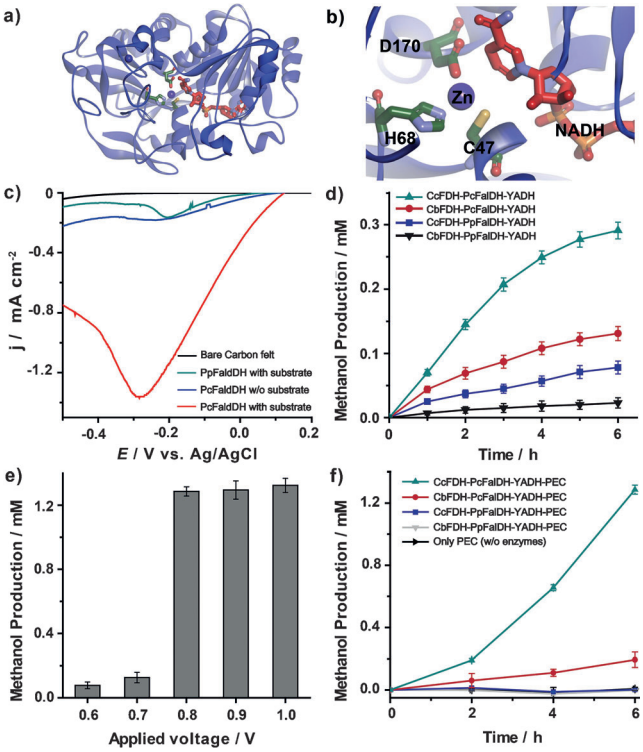

Figure 3. a) Homology model of PcFaldDH showing the catalytic residues (green sticks) and NADH. b) Active site pocket of PcFaldDH highlighting the catalytic residues (green color). The NADH and the catalytic Zn center in the active site pocket of the PcFaldDH are indicated. c) Comparison of the linear sweep voltammetry curves of bare carbon felt (black), PpFaldDH (green), and carbon felt with adsorbed PcFaldDH with (red) and without substrate (blue) at pH 7. d) Methanol production as a function of time in multienzymatic systems. The initial NADH concentration was 5 mM. e) Photoelectrochemical production of methanol by TPIEC under various applied potentials with illumination by visible light. The initial NAD^+ concentration was 5 mM. f) Methanol production of the TPIEC system as a function of time in various multienzymatic systems with an external voltage of 0.8 V.

Prior to applying the enzyme cascade system to the Co-Pi/α-Fe_2O_3 | $BiFeO_3$ tandem PEC system, we tested each enzyme with the NADH-regenerating PEC platform and confirmed that each biocatalytic redox reaction was induced by the generated NADH in the PEC system (see Figures S21—S23). Thereafter, we fabricated the TPIEC system by coupling the enzyme cascade with the NADH-regenerating PEC platform for the production of methanol. Solar-assisted, CO_2 to methanol conversion was performed for 6 h in the TPIEC system and analyzed by gas chromatography and NMR spectroscopy (Figure 3e, Figure S24).[15] Until the external applied voltage reached 0.8 V, only a small amount of methanol was detected; however, when more than 0.8 V was applied, photobiocatalytically produced methanol was obtained at a concentration of 1.31 mM with a faradaic efficiency of 31.9%. We attribute this significant increment to the NADH/NAD^+ ratio, which was dependent on the applied

voltage (see Figure S25). According to the literature,[16] the NADH/NAD$^+$ ratio significantly affects the catalytic performances of NADH-dependent enzymes. As the reactions catalyzed by these enzymes are reversible, the NADH/NAD$^+$ ratio is critical to the production of methanol in the biocatalytic PEC system. Figure S25 and Figure 2c show that the NADH/NAD$^+$ ratio increased substantially when the electrochemical bias reached 0.8 V and was only slightly enhanced after 0.8 V, consistent with the NADH generation profile. These results indicate an inefficiency in energy transfer at the high potential, which is in agreement with the significant decrease in EABPE above 0.8 V (Figure 2b). Furthermore, high voltages can induce the formation of byproducts in PEC systems.[17] The production of methanol by the TPIEC system in Figure 3e showed a similar profile as the NADH/NAD$^+$ ratio versus applied voltage (see Figure S25), and the optimal electrochemical bias for the biocatalytic synthesis of methanol through photoelectrochemical NADH regeneration was approximately 0.8 V. Hence, we performed subsequent experiments with a voltage of 0.8 V. We conducted several negative control experiments for each component of the TPIEC system (see Figure S26). According to our results, methanol was not synthesized at all in the absence of the enzymes, Rh complex **M**, or NAD$^+$, which indicates methanol was generated only through the three-enzyme cascade reactions. We noted that a small amount of formate (0.15 mM) was formed with **M** in the absence of enzymes and NAD$^+$ after incubation for 6 h, thus indicating that CO_2 can be partially reduced to formate by **M,** which was used for the generation of formate and coupled with a subsequent enzymatic reaction in recent studies.[15b,18] However, the amount of formate (2.03 mM) produced with CcFDH in the NADH-regenerating PEC system was less than 10% (see Figure S21). In addition, we carried out a control experiment of the TPIEC system without CcFDH. According to the result (see Figure S27), only small amounts of methanol (0.03 mM) and formate (0.11 mM) were synthesized relative to the full TPIEC system (Figures 3f and S26). These limited conversions indicate that most of the methanol was generated in the TPIEC system through the consecutive enzymatic reactions.

We investigated TPIEC systems with different multienzymatic combinations over 6 h (Figure 3f). When PcFaldDH was not involved in the multienzymatic cascade, the TPIEC systems failed to produce methanol. In the PcFaldDH-containing TPIEC systems, the replacement of CbFDH by CcFDH resulted in a 6.5-fold increase in the methanol concentration. Thus, the improved reduction of formate by PcFaldDH and the slow oxidation of formate by CcFDH led to the rapid and efficient reduction of CO_2 in the photobiocatalytic reaction system. We estimated the efficiencies for the conversion of CO_2 into methanol in the TPIEC system on the basis of the average rate of methanol formation per reaction volume (C_{avg}, $\mu M\,h^{-1}$) and photocatalyst weight (R_{avg}, $\mu mol\,g_{cat}^{-1}\,h^{-1}$). The calculated C_{avg} and R_{avg} values for the Co-Pi/α-Fe_2O_3 | $BiFeO_3$ tandem PEC cell integrated with the CcFDH-PcFaldDH-YADH enzyme cascade were 220 $\mu M\,h^{-1}$ and 1280 $\mu mol\,g_{cat}^{-1}\,h^{-1}$, respectively (Table 1). These values are high compared to other systems reported to date for the conversion of CO_2 into methanol by irradiation with visible light under ambient conditions based on photoenzymatic,[5] electroenzymatic,[19] photoelectrochemical,[20] and photochemical[21] pathways.

Table 1: Comparison of the efficiencies for the CO_2 to methanol conversion in various photocatalytic systems.

Category	Photocatalyst	Electron donor	C_{avg} [a]	R_{avg} [b]
this study	$BiFeO_3$	H_2O	220.0	1279.8
photoenzymatic	CCG-IP[5b]	TEOA	7.5	46.3
	Eosin Y[5c]	TEOA	6.0	186.4
photochemical, non-enzymatic	Bi_2WO_6[1f]	H_2O	107.1	75
	Au-Cu/graphene/Cu_2O[21a]	H_2O	586.7	–
	$NiO/InNbO_4$[21b]	H_2O	31.5	1.58
	carbon QD/Cu_2O[21c]	H_2O	98	56
	Bi_2S_3/CdS[21d]	H_2O	122.6	88
	$CdS/Bi_2S_3/TiO_2$[21e]	H_2O	44.9	44.9
	RuO_2/$Cu_xAg_yIn_zZn_kS_m$[21f]	H_2	118.5	118.5
	$NiO/InTaO_4$[21g]	H_2O	–	11.1

[a] Average rate of methanol formation per reaction volume, in $\mu M\,h^{-1}$.[20b,c] [b] Average rate of methanol formation per photocatalyst weight, in $\mu mol\,g^{-1}\,h^{-1}$.[21g] TEOA = triethanolamine.

In summary, we have demonstrated a PEC synergistic biocatalyzed conversion of CO_2 into methanol by the integration of an NADH-regenerating tandem PEC cell and a multienzyme cascade. The design of the iron oxide based, NADH-regenerating Co-Pi/α-Fe_2O_3 | $BiFeO_3$ tandem PEC cell was based on proper alignment of the band edges of two photoelectrodes and the internal electric field of a $BiFeO_3$ photocathode, which induced electron transfer to **M** and NAD$^+$. The tandem PEC cell utilized water as an electron donor and generated NADH from NAD$^+$ without electrical bias. The yield of NADH regeneration increased up to 80% at an applied bias of 0.8 V. For the efficient biocatalytic conversion of CO_2 into methanol, the superior formate-reducing ability of PcFaldDH was identified and exploited for the first time in a three-dehydrogenase cascade system. The combination of the NADH-regenerating PEC system and the CcFDH-PcFaldDH-YADH cascade system resulted in high efficiencies for methanol formation compared with other systems mediated by visible light. Overall, this two-system-integration approach is a promising strategy for the conversion of CO_2 into valuable chemicals with highly selectivity from inexpensive materials by using a PEC system and using readily available solar energy and water.

Acknowledgements

This study was supported by the National Research Foundation (Grant nos.: NRF-2015R1A3A2066191 and 2013M3A6A8073184) and the Samsung Research Funding Center of Samsung Electronics (Grant no.: SRFC-TA1403-01), Republic of Korea.

Conflict of interest

The authors declare no conflict of interest.

Keywords: biocatalysis · CO_2 reduction · enzymes · methanol production · photosynthesis

[1] a) N. S. Lewis, D. G. Nocera, *Proc. Natl. Acad. Sci. USA* **2006**, *103*, 15729 – 15735; b) E. E. Barton, D. M. Rampulla, A. B. Bocarsly, *J. Am. Chem. Soc.* **2008**, *130*, 6342; c) S. H. Lee, J. H. Kim, C. B. Park, *Chem. Eur. J.* **2013**, *19*, 4392 – 4406; d) J. H. Kim, D. H. Nam, C. B. Park, *Curr. Opin. Biotechnol.* **2014**, *28*, 1 – 9; e) D. Kim, K. K. Sakimoto, D. C. Hong, P. D. Yang, *Angew. Chem. Int. Ed.* **2015**, *54*, 3259 – 3266; *Angew. Chem.* **2015**, *127*, 3309 – 3316; f) L. Liang, F. Lei, S. Gao, Y. Sun, X. Jiao, J. Wu, S. Qamar, Y. Xie, *Angew. Chem. Int. Ed.* **2015**, *54*, 13971 – 13974; *Angew. Chem.* **2015**, *127*, 14177 – 14180; g) M. D. Porosoff, B. H. Yan, J. G. G. Chen, *Energy Environ. Sci.* **2016**, *9*, 62 – 73; h) E. J. Son, J. W. Ko, S. K. Kuk, H. Choe, S. Lee, J. H. Kim, D. H. Nam, G. M. Ryu, Y. H. Kim, C. B. Park, *Chem. Commun.* **2016**, *52*, 9723 – 9726.

[2] a) S. Kuwabata, K. Nishida, R. Tsuda, H. Inoue, H. Yoneyama, *J. Electrochem. Soc.* **1994**, *141*, 1498 – 1503; b) J. Graciani, K. Mudiyanselage, F. Xu, A. E. Baber, J. Evans, S. D. Senanayake, D. J. Stacchiola, P. Liu, J. Hrbek, J. F. Sanz, J. A. Rodriguez, *Science* **2014**, *345*, 546 – 550.

[3] a) S. N. Habisreutinger, L. Schmidt-Mende, J. K. Stolarczyk, *Angew. Chem. Int. Ed.* **2013**, *52*, 7372 – 7408; *Angew. Chem.* **2013**, *125*, 7516 – 7557; b) J. L. White, M. F. Baruch, J. E. Pander, Y. Hu, I. C. Fortmeyer, J. E. Park, T. Zhang, K. Liao, J. Gu, Y. Yan, T. W. Shaw, E. Abelev, A. B. Bocarsly, *Chem. Rev.* **2015**, *115*, 12888 – 12935.

[4] a) T. E. Rosser, C. D. Windle, E. Reisner, *Angew. Chem. Int. Ed.* **2016**, *55*, 7388 – 7392; *Angew. Chem.* **2016**, *128*, 7514 – 7518; b) H. Takeda, H. Koizumi, K. Okamoto, O. Ishitani, *Chem. Commun.* **2014**, *50*, 1491 – 1493.

[5] a) D. H. Nam, S. K. Kuk, H. Choe, S. Lee, J. W. Ko, E. J. Son, E. G. Choi, Y. H. Kim, C. B. Park, *Green Chem.* **2016**, *18*, 5989 – 5993; b) R. K. Yadav, G. H. Oh, N. J. Park, A. Kumar, K. J. Kong, J. O. Baeg, *J. Am. Chem. Soc.* **2014**, *136*, 16728 – 16731; c) X. Ji, Z. Su, P. Wang, G. Ma, S. Zhang, *Small* **2016**, *12*, 4753 – 4762.

[6] a) E. M. Nichols, J. J. Gallagher, C. Liu, Y. Su, J. Resasco, Y. Yu, Y. Sun, P. Yang, M. C. Chang, C. J. Chang, *Proc. Natl. Acad. Sci. USA* **2015**, *112*, 11461 – 11466; b) C. Liu, J. J. Gallagher, K. K. Sakimoto, E. M. Nichols, C. J. Chang, M. C. Chang, P. Yang, *Nano Lett.* **2015**, *15*, 3634 – 3639; c) T. Kothe, N. Plumere, A. Badura, M. M. Nowaczyk, D. A. Guschin, M. Rogner, W. Schuhmann, *Angew. Chem. Int. Ed.* **2013**, *52*, 14233 – 14236; *Angew. Chem.* **2013**, *125*, 14483 – 14486; d) P. Zhou, J. G. Yu, M. Jaroniec, *Adv. Mater.* **2014**, *26*, 4920 – 4935.

[7] a) K. Sivula, F. Le Formal, M. Gratzel, *ChemSusChem* **2011**, *4*, 432 – 449; b) J. Y. Kim, G. Magesh, D. H. Youn, J. W. Jang, J. Kubota, K. Domen, J. S. Lee, *Sci. Rep.* **2013**, *3*, 2681; c) D. H. Nam, G. M. Ryu, S. K. Kuk, D. S. Choi, E. J. Son, C. B. Park, *Appl. Catal. B* **2016**, *198*, 311 – 317.

[8] a) D. Cao, Z. Wang, Nasori, L. Wen, Y. Mi, Y. Lei, *Angew. Chem. Int. Ed.* **2014**, *53*, 11027 – 11031; *Angew. Chem.* **2014**, *126*, 11207 – 11211; b) W. Ji, K. Yao, Y. F. Lim, Y. C. Liang, A. Suwardi, *Appl. Phys. Lett.* **2013**, *103*, 062901; c) W. Ji, K. Yao, Y. C. Liang, *Adv. Mater.* **2010**, *22*, 1763; d) A. M. Glass, D. V. D. Linde, D. H. Auston, T. J. Negran, *J. Electron. Mater.* **1975**, *4*, 915 – 943.

[9] S. H. Lee, G. M. Ryu, D. H. Nam, J. H. Kim, C. B. Park, *ChemSusChem* **2014**, *7*, 3007 – 3011.

[10] a) A. J. Nozik, *Appl. Phys. Lett.* **1976**, *29*, 150 – 153; b) Y. H. Lai, D. W. Palm, E. Reisner, *Adv. Energy Mater.* **2015**, *5*, 1501668.

[11] J. Newman, *J. Electrochem. Soc.* **2013**, *160*, F309 – F311.

[12] a) Y. Li, W. Zhang, J. F. Niu, Y. S. Chen, *ACS Nano* **2012**, *6*, 5164 – 5173; b) X. J. Shi, Y. Choi, K. Zhang, J. Kwon, D. Y. Kim, J. K. Lee, S. H. Oh, J. K. Kim, J. H. Park, *Nat. Commun.* **2014**, *5*, 4775.

[13] a) S. L. Li, S. Freguia, S. M. Liu, S. S. Cheng, S. Tsujimura, O. Shirai, K. Kano, *Biosens. Bioelectron.* **2010**, *25*, 2651 – 2656; b) A. Bassegoda, C. Madden, D. W. Wakerley, E. Reisner, J. Hirst, *J. Am. Chem. Soc.* **2015**, *137*, 4592 – 4592.

[14] A. Alissandratos, H. K. Kim, H. Matthews, J. E. Hennessy, A. Philbrook, C. J. Easton, *Appl. Environ. Microbiol.* **2013**, *79*, 741 – 744.

[15] a) X. Y. Ji, Z. G. Su, P. Wang, G. H. Ma, S. P. Zhang, *ACS Nano* **2015**, *9*, 4600 – 4610; b) K. Ma, O. Yehezkeli, E. Park, J. N. Cha, *ACS Catal.* **2016**, *6*, 6982 – 6986; c) J. M. Saveant, C. Tard, *J. Am. Chem. Soc.* **2016**, *138*, 1017 – 1021.

[16] a) C. Zhang, K. Ma, X. H. Xing, *Int. J. Hydrogen Energy* **2009**, *34*, 1226 – 1232; b) J. Wang, Y. M. Kim, H. S. Rhee, M. W. Lee, J. M. Park, *Bioresour. Technol.* **2013**, *135*, 199 – 206; c) C. Zhang, F. X. Lv, X. H. Xing, *Bioresour. Technol.* **2011**, *102*, 8344 – 8349.

[17] a) J. L. Qiao, Y. Y. Liu, F. Hong, J. J. Zhang, *Chem. Soc. Rev.* **2014**, *43*, 631 – 675; b) A. S. Agarwal, Y. Zhai, D. Hill, N. Sridhar, *ChemSusChem* **2011**, *4*, 1301 – 1310.

[18] a) O. Yehezkeli, N. M. Bedford, E. Park, K. Ma, J. N. Cha, *ChemSusChem* **2016**, *9*, 3188 – 3195; b) M. B. Chambers, X. Wang, N. Elgrishi, C. H. Hendon, A. Walsh, J. Bonnefoy, J. Canivet, E. A. Quadrelli, D. Farrusseng, C. Mellot-Draznieks, M. Fontecave, *ChemSusChem* **2015**, *8*, 603 – 608.

[19] a) P. K. Addo, R. L. Arechederra, A. Waheed, J. D. Shoemaker, W. S. Sly, S. D. Minteer, *Electrochem. Solid-State Lett.* **2011**, *14*, E9 – E13; b) S. Schlager, L. M. Dumitru, M. Haberbauer, A. Fuchsbauer, H. Neugebauer, D. Hiemetsberger, A. Wagner, E. Portenkirchner, N. S. Sariciftci, *ChemSusChem* **2016**, *9*, 631 – 635.

[20] a) J. L. Yuan, P. C. Wang, C. J. Hao, G. C. Yu, *Electrochim. Acta* **2016**, *193*, 1 – 6; b) Z. X. Yang, J. F. Xu, C. X. Wu, H. Jing, P. Q. Li, H. Z. Yin, *Appl. Catal. B* **2014**, *156*, 249 – 256; c) P. Q. Li, J. F. Xu, H. Jing, C. X. Wu, H. Peng, J. Lu, H. Z. Yin, *Appl. Catal. B* **2014**, *156*, 134 – 140; d) J. L. Yuan, C. J. Hao, *Sol. Energy Mater. Sol. Cells* **2013**, *108*, 170 – 174; e) K. Rajeshwar, N. R. de Tacconi, G. Ghadimkhani, W. Chanmanee, C. Janaky, *ChemPhysChem* **2013**, *14*, 2251 – 2259.

[21] a) J. G. Hou, H. J. Cheng, O. Takeda, H. Zhu, *Angew. Chem. Int. Ed.* **2015**, *54*, 8480 – 8484; *Angew. Chem.* **2015**, *127*, 8600 – 8604; b) D. S. Lee, H. J. Chen, Y. W. Chen, *J. Phys. Chem. Solids* **2012**, *73*, 661 – 669; c) H. T. Li, X. Y. Zhang, D. R. MacFarlane, *Adv. Energy Mater.* **2015**, *5*, 1401077; d) X. Li, J. T. Chen, H. L. Li, J. T. Li, Y. T. Xu, Y. J. Liu, J. R. Zhou, *J. Nat. Gas Chem.* **2011**, *20*, 413 – 417; e) X. Li, H. L. Liu, D. L. Luo, J. T. Li, Y. Huang, H. L. Li, Y. P. Fang, Y. H. Xu, L. Zhu, *Chem. Eng. J.* **2012**, *180*, 151 – 158; f) J. Y. Liu, B. Garg, Y. C. Ling, *Green Chem.* **2011**, *13*, 2029 – 2031; g) Z. Y. Wang, H. C. Chou, J. C. S. Wu, D. P. Tsai, G. Mul, *Appl. Catal. A* **2010**, *380*, 172 – 177.

Manuscript received: November 21, 2016
Final Article published: ■■ ■■, ■■■■

Communications

Biocatalytic Photosynthesis

S. K. Kuk, R. K. Singh, D. H. Nam, R. Singh, J. K. Lee,* C. B. Park* _____ ■■■–■■■

Photoelectrochemical Reduction of Carbon Dioxide to Methanol through a Highly Efficient Enzyme Cascade

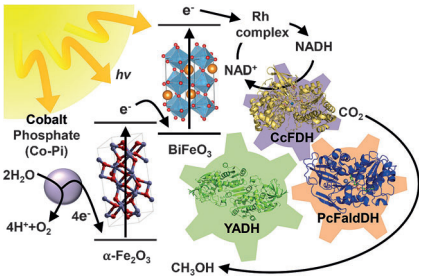

In synergy: A tandem photoelectrochemical (PEC) cell with an integrated enzyme cascade has been developed to transfer photogenerated electrons to a multienzyme cascade for the biocatalyzed reduction of CO_2 to methanol in high yield. The approach makes use of water as an electron donor, a hematite photoanode and a bismuth ferrite photocathode for the regeneration of NADH with visible light, as well as a three-dehydrogenase cascade system.